ABSTRACTING GIS LAYERS FROM HYPERSPECTRAL IMAGERY

Torsten E. Howard, Michael J. Mendenhall, and Gilbert L. Peterson

Department of Electrical & Computer Engineering
Air Force Institute of Technology
Wright-Patterson AFB, Ohio 45433

ABSTRACT

The spectral-spatial relationship of materials in a hyperspectral image cube is exploited to partially automate the creation of Geographical Information System (GIS) layers. The topological neighborhood preservation property of the Self Organizing Map (SOM) is clustered into six (partially overlapping) neighborhoods that are mapped into the image domain to locate in-scene structures of similar material type. GIS layers are abstracted through spatial logical and morphological operations on the six image domain material maps and a novel road finding algorithm connects road segments under significant tree-occlusion resulting in a contiguous road network. It is assumed that specific knowledge of the scene (e.g. endmember spectra) *is not* available. The results are eight separate high-quality GIS layers (Vegetation, Trees, Fields, Buildings, Major Buildings, Roadways, and Parking Areas) that follow the scene features of the hyperspectral image and are separately and automatically labeled. The material maps resulting from clustering the SOM have an 84.3% average accuracy, which increases to 93.9% after spatial processing into GIS layers.

***Index Terms*—** Geographic Information Systems, Hyperspectral Image Processing, Hyperspectral, Self-Organizing Map, Morphological

1. INTRODUCTION

Geographical Information Systems (GISs) use layers of vector data (shape files) to represent features in a scene. The often manual process begins with an orthorectified RGB image and outlines spatial features of interest. The resulting layers are then viewed independent of the imagery providing an abstraction of the scene that is often more usable to the observer than the original image itself.

The previously described manual process is prone to human error and is time consuming. Time and cost considerations limit feature shapes to regular polygons and result in a slow update cycle. The manual effort is further complicated by scene clutter leaving the abstraction open to interpretation. In order to verify the results, ground truth data is collected by visiting the area of interest. As new imagery is collected and orthorectified, existing shape files are often manually adjusted and updated to reflect cumulative scene changes. As stated in [1], "'. . . the biggest challenge is the currency of data, the authenticity of data,' and the primary complaint is 'that's not my house'".

Hyperspectral imagery, with its high spectral fidelity, holds the possibility of partially or fully automating and significantly improving this process, reducing time and cost of creating shape files, and increasing the quality of the feature outlines. Special attention needs to be paid to the road network, and as noted in [2], ". . . primarily in urban areas the concern is with the road pattern, as this determines the framework in which the complexities of urban land use change usually take place."

This work combines both spectral and spatial analysis of hyperspectral imagery to automate shape file generation. The expectation is that our automated process will reduce human error, increase shape files creation rate, increase fidelity of shapes from simple polygons to more meaningful feature outlines, and close the shape file / imagery gap as shape files are derived directly from the hyperspectral image.

1.1. Spectral Analysis

A myriad of approaches exist for clustering hyperspectral data. Two notable unsupervised clustering methods are K-means clustering and Kohonen's Self-Organizing Map (SOM) [3]. Spectral analysis with K-Means clustering poses several challenges. The most notable are determining the number of clusters K and spatially connecting the results. K-Means clustering is used to spectrally cluster pixels in [4], where K was varied from 2–16 yielding 101–695 separate spatial regions. Connecting these regions into meaningful abstractions that are separately labeled is an insurmountable task.

The SOM offers a more meaningful spectral clustering and provides an intuitive mechanism for mapping spectral clusters to the spatial image domain. Examples of this by the authors in [5] visualize the clustering of the SOM neighborhood topology and the corresponding image domain representation. Data in the SOM are organized on a two-dimensional lattice of *processing elements* (PEs). Each PE has associated with it a prototype vector that is a quantization of the data. One may consider the representation of the SOM as having "pure" spectra mapped to given SOM PEs and mixed spectra mapped to PEs between the pure spectra. This produces distinguishable regions that can be correlated with specific materials of interest (MOIs). By identifying the regions on the SOM lattice and mapping them to the spatial domain, a binary spatial image material map can be developed which identifies the location of each material. This spectral-to-spatial mapping is reliable due to the global ordering and topological preservation properties of the SOM. These material maps are the basis for the spatial analysis using logical and morphological operations.

1.2. Spatial Analysis

Morphological *close* and *open* operations performed on the material maps with a known structuring element (SE) result in GIS layers. A SE is a binary valued matrix that can be as small as a (1×2) or (2×1). The SE, similar to a sliding window, selects every subset of the material map equal in spatial size to the SE. The SE size is chosen to correspond to the minimum scene feature sizes (e.g., where a minimum building size of 3×3 pixels prescribes a 3×3

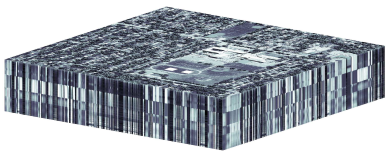

Fig. 1. Synthetic hyperspectral image cube.

SE). The morphological open and close operations are used in two ways: to improve aesthetic appeal of the GIS layers; and to isolate larger features (e.g., fields). A morphological close fills in the space between pixels clustered in an area smaller than the size of the SE. An open deletes pixels smaller than the size of the SE. Iterative open and close operations with a SE that increases in each dimension by one during each iteration isolates larger scene features.

Morphological operations perform similar to a conceptual understanding of a scene as an observer sees it. That is, when a person views a binary image, the tendency is to cluster close-lying pixels (a morphological close) into recognizable shapes, and to ignore speckle and other artifacts (a morphological open) that have no distinguishable shape or order.

2. METHODOLOGY

The scene used in this work is a 400×400 pixel synthetic hyperspectral image cube with 194 spectral bands in the range 397.5 – $2480.2nm$ shown in Fig. 1. The image is resampled spectrally to reflect a NASA/JPL AVIRIS-acquired image. It is atmospherically corrected using the empirical line method and irrecoverably lost spectra due to atmospheric water absorption are removed.

2.1. Self Organizing Map

The process begins with a clustering of the hyperspectral image using a SOM where the learning parameters are specified in Table 1. The Normalized Difference Vegetative Index (NDVI) and exemplars from building roofs and roadways seed the algorithm to cluster the SOM neighborhoods and label PEs with a material type. An example of three SOM clustered regions is shown in Fig. 2(a).

2.2. Vegetation Shape File

Vegetation PEs are identified by way of the NDVI expressed in Eq. 1 where RED is the average of the bands between 580nm and 690nm and NIR is the average between 725nm and 1100nm. The vegetation region of the SOM is the green area shown in Fig. 2(a) where a threshold of NDVI > 0.3 is applied to the SOM PEs. This region is next divided into tree and non-tree vegetative regions.

$$\text{NDVI} = \frac{\text{NIR} - \text{RED}}{\text{NIR} + \text{RED}} \tag{1}$$

2.3. Tree Shape File

Broad-leaf trees are a subset of vegetation segmented using the standard deviation of the near-infrared scatter normalized between 950 and 1250nm. The standard deviation is thresholded at a value of 0.2 where values above that threshold are declared as trees, the results of which are shown in Fig. 2(b). The resulting material map for trees is shown in Fig. 2(c). To improve aesthetic appeal, the tree map is closed with a 3×3 SE producing the results in Fig. 2(d). The size of the SE is chosen to correspond with the minimum tree size given a spatial resolution of $\approx 1.5m/$pixel.

Table 1. SOM learning parameters

Parameter	Value
Size	40×40 PEs
Initial / final learn rates	$\alpha = 0.8$ / $\alpha = 5 \times 10^{-4}$
Initial / final neighborhood widths	$\sigma = 1.0$ / $\sigma = 5 \times 10^{-4}$
Training steps	6×10^6

2.4. Non-Tree Vegetation and Fields Shape Files

The non-broad-leaf tree vegetative region shown in Fig. 2(e) results when the tree region in Fig. 2(b) is logically deleted from the green vegetation region show in Fig. 2(a). The associated material map shown in Fig. 2(f) consists primarily of grasses. A field is defined as having a spatial area between 5×5 and 24×24 pixels, which prescribes the SE size. The fields shape file is generated by performing 20 iterative open/close morphological operations while increasing the SE by one in each dimension from the minimum (5×5) to the maximum size (24×24). The final step is to logically remove the road network shape file shown in Fig. 2(p) (created later in Sec. 2.7). The final fields shape file (less road network) is shown in Fig. 2(g).

The final non-tree vegetation shape file shown in Fig. 2(h) is created by logically deleting three shape files from the vegetation material map in Fig. 2(f) and then performing a morphological close with a 3×3 SE for aesthetic appeal. The three shape files are the tree shape file in Fig. 2(d), the final buildings shape file in Fig. 2(k) (created later in Sec. 2.5) and the road network shown in Fig. 2(p) (from Sec. 2.7).

2.5. Buildings and Major Buildings Shape Files

To create the builidngs shape file, the ℓ_2–norm between an exemplar rooftop spectra (manually) selected from the hyperspectral image and each PE's weight vector is computed. The distances are thresholded using a value of 2 generating the segmentation of the SOM shown in Fig. 2(i). This segmentation is used to create the rooftop material map in Fig. 2(j).

The maps in Figs. 2(f,g) and Figs. 2(n,o) (created later) are logically added to create a *negative image mask* (NIM) shown in Fig. 3(a) indicating where buildings are *not* located. The inverse of the NIM is added to the rooftop material map from Fig. 2(j) (also shown in Fig. 3(b)) resulting in the buildings map in Fig. 3(c) which is then morphologically opened with a 3×3 SE resulting in Fig. 3(d). The minimum building size is $\approx 3 \times 3$ which prescribes the SE size. Finally, the road network from Fig. 2(p) (created later) is logically removed resulting in in the building shape file in Fig. 2(k).

A major building is (arbitrarely) defined as five times the area of a typical small building (e.g., a large shed) giving way to a 7×7 pixel region. As such, the buildings shape file shown in Fig. 3(d) is opened with a 7×7 SE deleting smaller building structures. A morphological dilation using a 5×5 SE followed by a morphological close using a 3×3 SE produces the major buildings shape file in Fig. 2(l). For aesthetic appeal, the dilation increases the size of the major buildings to make them more prominent, and the close ensures the shapes are without visual distractions from missing pixels.

2.6. Parking Lots Shape File

Exemplar roadway spectra from the hyperspectral image as used in Sec. 2.5 determines the SOM region in Fig. 2(m) and the roadway material map in Fig. 2(n). Parking areas are defined as having a spatial area between 2×2 and 10×10 pixels, which prescribes the

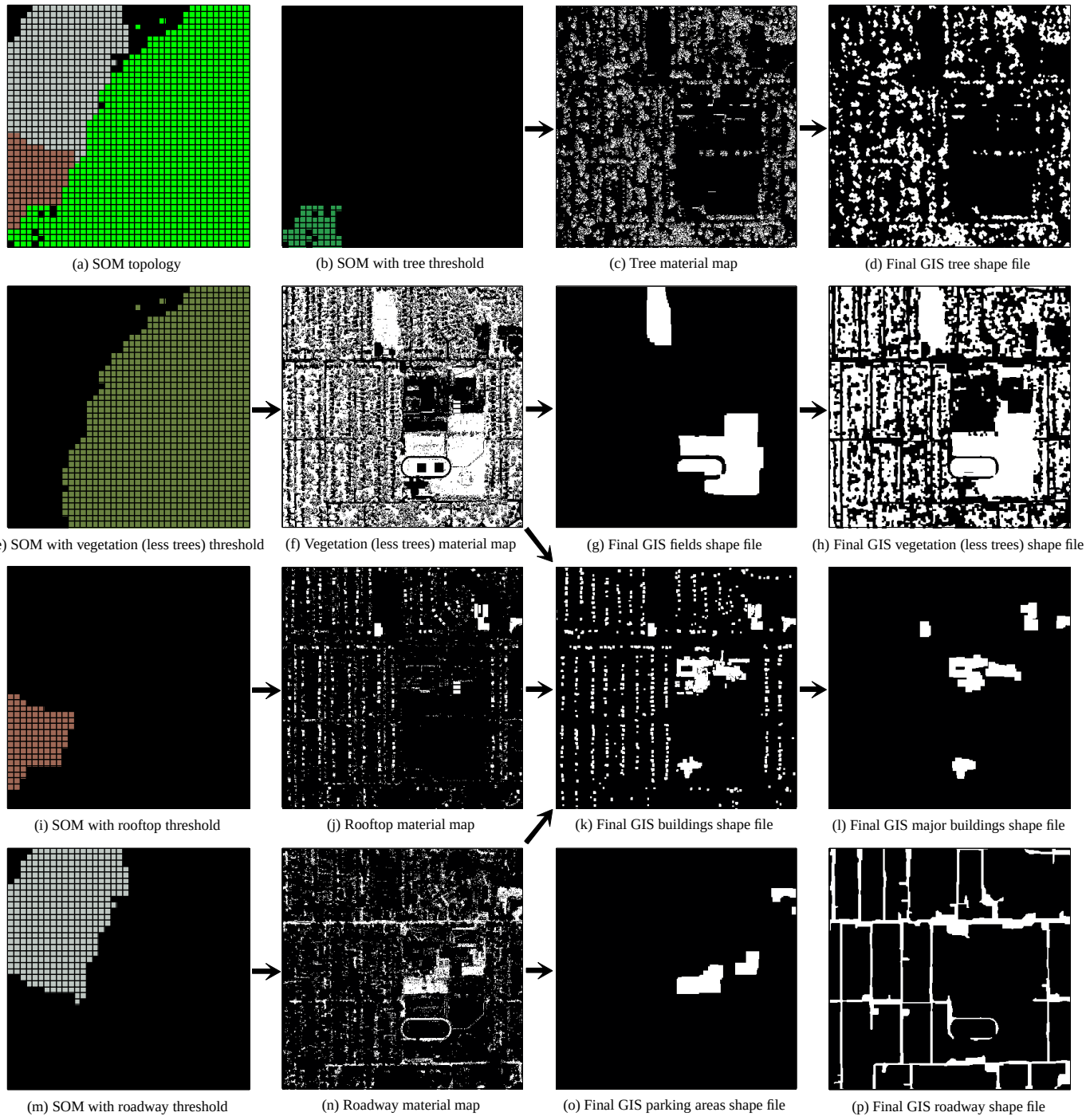

Fig. 2. A pictorial view of the process presented in this work that generates GIS shape files from a hyperspectral image cube.

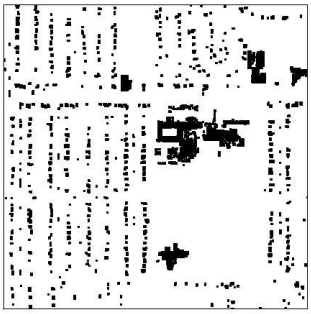

(a) Negative image mask (NIM)

(b) Rooftop material map

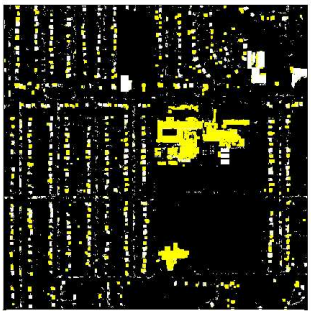

(c) Rooftop map (white) and NIM (yellow)

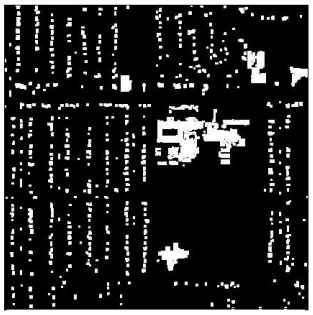

(d) After morphological open (3×3 SE)

Fig. 3. Process to create the buildings shape file.

(a) False color composite

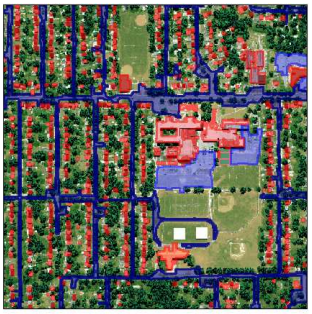

(b) Road network, parking areas, and buildings

(c) Vegetation (less trees) and fields

(d) Trees

Fig. 4. False color composite and final GIS layers.

SE size. The iterative morphological open/close method described in Sec. 2.4 (used to abstract the fields shape file) is used on the roadway material map from Fig. 2(n) to produce the parking areas shape file in Fig. 2(o).

2.7. Roadway Shape File

The roadway shape file results from a novel road finding algorithm that requires a reduced roadway material map, a NIM, and a maximum NIM threshold. The reduced material map results after performing a morphological open operation with a 3×3 SE on the roadway material map from Fig. 2(n) and logically deleting Figs. 2(f,g,l,o) and Fig. 3(d). The SE size prevents roads in this scene, which are two-lane roads and typically on the order of 4-5 pixels wide (roughly 6-7.5m), from being deleted. Possible non-road network pixels less than the SE size are removed (e.g. driveways). A NIM is constructed as in Sec. 2.5 with Figs. 2(f,g,l,o) and Fig. 3(d).

The road finding algorithm operates iteratively. During each iteration, it considers every pair of roadway pixels and compares the number of NIM pixels between them to the NIM threshold. The NIM threshold starts at 0 and is incremented to some maximal value (8 in this work). When the maximum threshold is reached, the algorithm logically removes the buildings shape file, Fig. 3(d), from the NIM, resets the NIM threshold to 0, and iterates. The road finding algorithm requires an experimentally determined 16 iterations, resulting in the GIS roadway shape file presented in Fig. 2(p).

3. RESULTS & CONCLUSION

Eight specific GIS shape files – Fields, Trees, Vegetation, Non-Tree Vegetation, Buildings, Major Buildings, Roadways, and Parking Areas – are abstracted from the hyperspectral image. Six are presented in Fig. 3. Spectral analysis resulted in an 84.3% average accuracy increasing to 93.9% (as compared with ground truth) after spatial analysis with logical and morphological operations. It is important to understand that the resulting shape files are *not* intended to be a pixel-for-pixel representation of the ground truth and we did not maximize the pixel-level classification. Rather, the process is designed for the qualitatively excellent understanding of the scene to a human observer as demonstrated in Fig. 4.

4. DISCLAIMER

The views expressed in this thesis are those of the author and do not reflect the official policy or position of the United States Air Force, Department of Defense, or the United States Government.

5. REFERENCES

[1] K2 Climb and Explorersweb, "Alpine style in science, solar panels in space, google maps and the japanese man," May 2006.

[2] Merrill K. Ridd and James D. Hipple, Eds., *Remote Sensing of Human Settlements*, vol. 5, American Society for Photogrammetry and Remote Sensing, 3 edition, 2006.

[3] T. Kohonen, *Self-Organizing Maps*, Springer-Verlag, Berlin, Germany, 1995.

[4] A. W. Meyer, D. W. Paglieroni, and C. Astaneh, "K-means re-clustering algorithmic options with quantifiable performance comparisons," *The International Society for Optical Engineering, Photonics*, January 2003.

[5] K. Tasdemir and E. Merenyi, "Exploiting data topology in visualization and clustering of self-organizing maps," *IEEE Transactions on : Accepted for future publication Neural Networks*.